The Journal of Experimental Biology 215, 2586-2600

doi:10.1242/jeb.064733

RESEARCH ARTICLE

Sensory receptor diversity establishes a peripheral population code for stimulus duration at low intensities

Ariel M. Lyons-Warren, Michael Hollmann and Bruce A. Carlson*

Department of Biology, Washington University in St Louis, Campus Box 1137, One Brookings Drive, St Louis, MO 63130-4899, USA

*Author for correspondence (carlson.bruce@wustl.edu)

SUMMARY

Peripheral filtering is a fundamental mechanism for establishing frequency tuning in sensory systems. By contrast, detection of temporal features, such as duration, is generally thought to result from temporal coding in the periphery, followed by an analysis of peripheral response times within the central nervous system. We investigated how peripheral filtering properties affect the coding of stimulus duration in the electrosensory system of mormyrid fishes using behavioral and electrophysiological measures of duration tuning. We recorded from individual knollenorgans, the electrosensory receptors that mediate communication, and found correlated variation in frequency tuning and duration tuning, as predicted by a simple circuit model. In response to relatively high intensity stimuli, knollenorgans responded reliably with fixed latency spikes, consistent with a temporal code for stimulus duration. At near-threshold intensities, however, both the reliability and the temporal precision of responses decreased. Evoked potential recordings from the midbrain, as well as behavioral responses to electrosensory stimulation, revealed changes in sensitivity across the range of durations associated with the greatest variability in receptor sensitivity. Further, this range overlapped with the natural range of variation in species-specific communication signals, suggesting that peripheral duration tuning affects the coding of behaviorally relevant stimuli. We measured knollenorgan, midbrain and behavioral responses to natural communication signals and found that each of them were duration dependent. We conclude that at relatively low intensities for which temporal coding is ineffective, diversity among sensory receptors establishes a population code, in which duration is reflected in the population of responding knollenorgans.

Supplementary material available online at http://jeb.biologists.org/cgi/content/full/215/15/2586/DC1

Key words: mormyrid, weakly electric fish, duration tuning, electroreception, temporal coding, peripheral filtering, sensory processing.

Received 22 November 2011; Accepted 24 March 2012

INTRODUCTION

Sensory processing involves the detection of multiple stimulus features in what can generally be considered a two-step process: peripheral filtering followed by central computation. For example, in auditory systems, frequency tuning is first established by peripheral filtering, whereas tuning to temporal features of sounds such as interaural time differences (Köppl, 2009), duration (Aubie et al., 2009) and interval (Edwards et al., 2007; Edwards et al., 2008) are thought to arise from central computations. Similarly, peripheral electroreceptors in weakly electric fish are frequency tuned (Hopkins, 1976; Hopkins, 1981), whereas tuning to temporal features is generally thought to arise within central electrosensory pathways (Fortune et al., 2006). However, these central computations are based on peripheral responses, which can vary in relation to frequency tuning as well as other variables. Good examples include the need to resolve phase ambiguity when trying to localize sounds using interaural time differences by integrating across frequency channels (Peña and Konishi, 2000), and the detection of 'phantom' phase differences owing to amplitude-dependent latency shifts in weakly electric fishes (Carlson and Kawasaki, 2006; Carlson and Kawasaki, 2007). In the present study, we directly addressed how diversity among peripheral electrosensory receptors affects the coding of temporal information in the African mormyrid electric fish *Brienomyrus brachyistius*.

The electrosensory systems of weakly electric fishes are excellent model systems for studying temporal processing by sensory systems (Fortune et al., 2006; Rose, 2004; Sawtell et al., 2005; Zakon, 2003). Mormyrids emit a pulse-type electric organ discharge (EOD) for use in communication (Carlson, 2006) and active electrolocation (von der Emde, 1999). The EOD waveform is species specific (Hopkins, 1981). Temporal features of the EOD, particularly duration, play an important role in species recognition and mate choice (Arnegard et al., 2006; Feulner et al., 2009; Hopkins and Bass, 1981; Machnik and Kramer, 2008). In *B. brachyistius*, the EOD is composed of three phases: an initial, head-negative phase (P0) of relatively small amplitude, followed by a head-positive phase (P1) and finally a head-negative phase (P2) (Carlson et al., 2000).

Electric communication in mormyrids is mediated by a dedicated electrosensory pathway (Bell and Grant, 1989; Xu-Friedman and Hopkins, 1999). Electroreceptors called knollenorgans (KOs) respond to outside-positive changes in electrical potential with a fixed latency spike (Bennett, 1965; Hopkins and Bass, 1981). Primary afferent fibers synapse in the hindbrain nucleus of the electrosensory lateral line lobe (nELL) (Bell and Grant, 1989). From the nELL, bilateral projections are sent to a midbrain region, the anterior exterolateral nucleus (ELa), which projects ipsilaterally to the adjacent posterior exterolateral nucleus (ELp) (Carlson, 2009; Friedman and Hopkins, 1998; Szabo et al., 1983).

Hopkins and Bass (Hopkins and Bass, 1981) proposed a temporal code for EOD duration, in which different KOs respond to either the start or the end of an EOD because of differences in stimulus

polarity on opposite sides of the body. Duration information would then be extracted by comparing spike latency differences within the central KO pathway, most likely within ELa (Mugnaini and Maler, 1987; Friedman and Hopkins, 1998). However, KOs are not simply edge detectors. They are broadly tuned to frequencies that roughly correspond to the power spectrum of the species-specific EOD (Hopkins, 1981). Notably, frequency tuning differs among KOs (Arnegard et al., 2006), revealing that the peripheral coding of electrosensory stimuli varies across the population of receptors. In the present study, we asked how the diversity of KOs influences the peripheral coding of stimulus duration.

MATERIALS AND METHODS

Study species

We used individuals of both sexes of the weakly electric mormyrid fish *Brienomyrus brachyistius* (Gill 1862). Individuals ranged from 5.3 to 17.0 cm in standard length. Fish were purchased from commercial distributors and housed in community aquariums at a temperature of 26–28°C and a conductivity of 200–400 μS cm^{-1}, with a 12 h:12 h light:dark cycle. Fish were fed live black worms four times per week. All procedures were in accordance with guidelines established by the National Institutes of Health (NIH) and were approved by the Animal Care and Use Committee at Washington University in St Louis.

Knollenorgan recording

We anesthetized fish in 300 mg l^{-1} tricaine methanesulfonate (MS-222) (Sigma-Aldrich, St Louis MO, USA). We then immobilized and electrically silenced fish with 20–100 μl of 0.3 mg ml^{-1} gallamine triethiodide (Sigma-Aldrich). Once immobilized, the fish were submerged in a 12.5×20×45 cm chamber filled with freshwater, and placed on a platform with lateral supports. Aerated freshwater was gravity fed to the fish through a pipette tip placed into the mouth. Fish generally recovered from anesthesia within 15 min of freshwater respiration. We forged electrodes from borosilicate capillary glass (o.d.=1 mm, i.d.=0.5 mm; A-M Systems, Everett, WA, USA) using a Bunsen burner to bend the last 1 cm to a 30 deg angle and polish the tip. Tip inner diameter was 0.5 mm. The mean (±s.e.m.) resistance for five representative electrodes was 0.4±0.1 MΩ. The electrode was filled with tank water, connected to the headstage of a DC amplifier (A-M Systems model 1600), and then placed over, but not touching, individual KOs. Electrical activity was amplified 10×, digitized at 195.3 kHz (Tucker-Davis model RP2.1, Tucker-Davis Technologies, Alachua, FL, USA) and saved to disk using custom-made software (MATLAB 7.4, The MathWorks, Natick, MA, USA).

Constant-current stimuli were delivered by the amplifier through the electrode using bridge balance to minimize artifact (Arnegard et al., 2006). Stimuli were generated in MATLAB. Sinusoidal stimuli ranged from 0.1 to 30 kHz and consisted of 90 ms bursts with 5 ms cosine-squared on and off ramps. Monophasic positive and negative square-pulse stimuli ranged from 0.01 to 5 ms. Natural and manipulated EOD waveforms were generated in MATLAB using previously recorded waveforms. Stimuli were digital-to-analog converted (Tucker-Davis model RP2.1) and then attenuated (Tucker-Davis model PA5) prior to delivery. Threshold intensity was defined as the minimum stimulus intensity required to elicit an increased response relative to an equal duration reference window. Reference and response windows were 90 ms for sine waves and 20 ms for square pulses and natural waveforms. Because of the difference in window duration, which was necessary to accurately accommodate the different stimulus types, and the desire to quantify the time-locked edge response to square pulses, we used slightly different response criteria for the different types of stimuli. For sine-wave stimuli, a positive response constituted at least one more spike per repetition in the response window relative to the reference window across 15 repetitions. For square-pulse and natural-waveform stimuli, spikes from 25 repetitions were binned into 200 μs bins and a response was positive if the highest bin in the response window was greater than the highest bin in the reference window.

For frequency tuning curves, we determined the best frequency (BF; frequency with the lowest threshold) and the bandwidth (BW_{10}), measured as the difference between upper and lower frequencies with thresholds 10 dB above the threshold at the BF, based on logarithmic extrapolation between adjacent data points. We fit duration tuning curves to the equation:

$$I_t = \frac{a}{1 - e^{\left(-\frac{d}{\tau}\right)}}, \quad (1)$$

where I_t is the threshold intensity, d is stimulus duration, and a and τ are the asymptote and time constant, respectively, of the exponential decrease in threshold as a function of duration. Duration tuning curves using monophasic square pulses are equivalent to the strength–duration curves historically used to study neuronal excitability (Neumann and Nachmansohn, 1975).

To investigate the effect of stimulus intensity on KO response latency and frequency, we tested six square pulse durations (0.01, 0.05, 0.1, 0.5, 1 and 3 ms) across a range of intensities, from below threshold to above saturation. This range was approximately 20 dB, but varied for each KO and duration. We calculated the relative probability of response by subtracting the number of spikes in a 3 ms reference window immediately before the stimulus from the number of spikes in the 3 ms response window starting with the stimulus, and dividing by the number of repetitions (100). We calculated the first spike latency by identifying the time of the first spike within a 3 ms response window from the start of the stimulus for each repetition and then taking the mean of these times. Repetitions with no spike in the 3 ms window were excluded from the first spike latency calculation. From these first spike latencies, we calculated standard deviation as a measure of variability in first spike latency (i.e. jitter).

Modeling

To investigate the relationship between frequency and duration tuning, we modeled KOs using a simple electrical circuit (Bennett, 1965; Bennett, 1971). We started with a leaky integrate-and-fire neuron modeled as resistance (R_m) and capacitance (C_m) in parallel (Gabbiani and Koch, 1998). To this we added a series capacitance (C_s) component to represent the contributions of the epithelial plug that covers the sensory cells, the layers of epithelial cells in the wall of the receptor canal and the apical surface of the receptor cells (Szabo, 1965; Harder, 1968b; Zakon, 1986). We also added a parallel resistance component to represent skin resistance (R_s), resulting in voltage drops across the skin (V_s) and across the receptor (V_m) (Fig. 3A, inset).

In response to current, C_s will act as a high-pass filter of V_m whereas C_m will act as a low-pass filter of V_m. The total current, I, will be divided equally between R_s and C_s. Following Ohm's law, the resulting voltage changes across R_s and C_s are described in Eqn 2:

$$I = \frac{(V_s + V_m)}{R_s} + C_s\left(\frac{dV_s}{dt}\right). \quad (2)$$

First, the term representing the current across R_s is moved using algebraic rearrangement. All current passing through C_s will then

be divided across R_m and C_m. Thus, that term in the equation can be further broken down, again following Ohm's law, as shown in Eqn 3:

$$I - \frac{(V_s + V_m)}{R_s} = \frac{V_m}{R_m} + C_m\left(\frac{dV_m}{dt}\right). \quad (3)$$

Further algebraic rearrangement yields the following difference equations:

$$\left(\frac{dV_s}{dt}\right) = \left(\frac{1}{C_s}\right)\left[I - \frac{V_s}{R_s} - \frac{V_m}{R_s}\right], \quad (4)$$

$$\left(\frac{dV_m}{dt}\right) = \left(\frac{1}{C_m}\right)\left[I - \frac{V_s}{R_s} - \frac{V_m}{R_s} - \frac{V_m}{R_m}\right]. \quad (5)$$

We varied C_s and C_m from 0.005 to 1 nF and R_s and R_m from 1 to 10 MΩ and measured the input current required for V_m to reach an arbitrary voltage threshold (1 mV) as a function of sine-wave frequency and square-pulse duration (same stimuli used for KO recordings). The goal of this modeling was to assess the nature of the relationship between frequency tuning and duration tuning, and then determine whether a similar relationship was found for actual KOs.

Midbrain evoked potential recording

To measure evoked field potentials in ELa and ELp, we prepared fish for surgery by anesthetizing them in 300 mg l^{-1} MS-222 and then immobilizing them with 100–300 µl of a 3 mg ml^{-1} solution of gallamine triethiodide. Fish were then moved to a recording chamber and submerged, except for a small region of the dorsal surface of the head. Lidocaine (0.4%) was used as a local anesthetic and general anesthesia was maintained throughout the surgery by respirating fish with 100 mg l^{-1} MS-222. After removing the skin and securing a post to the skull, an area of bone was removed to expose the ELa and the ELp as described previously (Carlson, 2009). Once the surgery was complete, we switched respiration to aerated freshwater to bring the fish out of general anesthesia. We used a pair of electrodes placed next to the caudal peduncle to monitor the EOD command. This signal was amplified 1000× on a differential A-C amplifier (A-M Systems model 1700) and sent to a window discriminator (World Precision Instruments SYS-121, Sarasota, FL, USA) to detect EOD command times. The EOD command triggers inhibition of the KO pathway in nELL (Bell and Grant, 1989). Therefore, any repetition in which the fish emitted a command 2 to 5 ms before the stimulus was ignored.

Recording electrodes (o.d.=1.2 mm, i.d.=0.68 mm; A-M Systems model 62700) were pulled on a Flaming/Brown micropipette puller (Sutter Instrument Company model P-97, Novato, CA, USA), broken to a tip diameter of 10–15 µm and filled with 3 mol l^{-1} NaCl (resistance <100 kΩ). Evoked potentials from ELa and ELp were amplified 1000× and band-pass-filtered from 0.1 Hz to 5 kHz with a differential AC amplifier (A-M Systems model 1700), digitized at 97.6 kHz (Tucker-Davis model RX8), averaged and saved to disk using a custom MATLAB program. Evoked field potentials were identified based on their characteristic shape and timing (Amagai, 1998; Carlson, 2009; Szabo et al., 1979).

We delivered transverse electrosensory stimuli using electrodes located on the sides of the tank. Square pulses were generated by an isolated square pulse generator (A-M Systems model 2100) and attenuated before delivery (Hewlett Packard 350D, Palo Alto, CA, USA). Natural and manipulated EOD waveforms were generated in MATLAB, delivered by a signal processor (Tucker-Davis model RX8), attenuated (Tucker-Davis model PA5) and then isolated from ground (A-M Systems model 2200). Stimulus intensities are reported in mV cm^{-1} as measured at the location where fish were placed, in the absence of a fish. To measure evoked potential thresholds, we presented a single stimulus at a range of intensities and recorded the mean potential in response to 20 repetitions for natural/manipulated EODs or 40 repetitions for square pulses. We scored trials as responses when the mean potential exceeded three s.d. above or below the baseline mean. Three s.d. was chosen to encompass all of the variation observed during the 50 ms baseline pre-stimulus recording period. We adjusted the stimulus intensity in 1 dB steps until we identified the least intense signal that yielded a response. This stimulus intensity was considered the threshold. To measure the magnitude of responses to isointensity stimulation, we calculated the total area of the response. The area of the response was calculated using the sum of all points in the evoked potential (after subtracting the baseline mean) rather than the peak potential to capture differences in both duration and amplitude in a single measure. Importantly, this measure of total response area is not affected by the stimulus artifact because the upward and downward edges give rise to symmetrical positive and negative areas, respectively, which cancel each other out. Responses were then normalized to the largest response across all durations tested within that particular brain nucleus within a given fish to account for variation in the amplitude and duration of evoked potentials in ELa and ELp, as well as to control for differences in evoked potential responses that are due to fish size or electrode placement. Normalizing the values in this way allowed us to directly compare differences in response magnitude with respect to variation in stimulus duration.

Behavioral playback

Fish were isolated in a 20 l aquarium and confined to a PVC enclosure (20×3.5×3.5 cm) using netted end-caps (see Carlson et al., 2011). Uniform electric stimuli were presented to the fish using two 7.6 cm chlorided silver wires running along the inside of the sidewalls of the enclosure, with recording electrodes on each end of the enclosure. Square pulse stimuli were generated by an isolated square pulse stimulator (A-M Systems model 2100) followed by attenuation (Hewlett Packard 350D). We chose both monophasic and biphasic square pulses because behavioral responses to monophasic square pulses could be influenced by responses from ampullary receptors to the DC components of this signal (Bennett, 1965; Zakon, 1986). Natural and manipulated EOD waveforms were generated using a custom MATLAB program, delivered at 97.6 kHz (Tucker-Davis model RX8), attenuated (Tucker-Davis model PA5) and then isolated from ground (A-M Systems model 2200). Stimulus intensities are reported in mV cm^{-1} as measured from the center of the recording chamber in the absence of a fish. Recorded signals were amplified 100× and band-pass-filtered from 0.1 Hz to 20 kHz with a differential AC amplifier (A-M Systems model 1700). Recordings were digitized at 97.6 kHz (Tucker-Davis model RX8) and custom MATLAB software was used to mark EOD times of occurrence relative to stimulus times.

EOD rates were estimated by convolving EOD times with a 300 ms Gaussian filter (Carlson and Hopkins, 2004; Szűcs, 1998) and averaging responses to 20 repetitions of the stimulus (inter-stimulus intervals were 20 s). To minimize habituation, fish were allowed 1 min of rest between each trial. To determine behavioral thresholds, we calculated a baseline mean ± s.d. during the 5 s preceding a stimulus. We defined responses to stimuli as recordings

in which the mean EOD rate exceeded two s.d. above the baseline mean within 500 ms after stimulus presentation. We adjusted stimulus intensity in 1 dB steps until we identified the least intense signal that yielded a response. This stimulus intensity was considered the threshold. The discharge rate of mormyrids can be highly variable (Carlson, 2002). Therefore, to avoid false-positive responses, trials were repeated if the trace exceeded two s.d. during the baseline period before the stimulus; to avoid false-negative responses, trials were repeated if the s.d. was greater than 1.5 EODs s^{-1}.

To measure isointensity responses, 15 or 20 stimulus repetitions were presented in 20 s intervals. For square pulses, each trial was repeated three times and then averaged. From the average of all trials, we defined the duration of the response as the time from when the EOD rate first crossed two s.d. above the baseline mean until it recrossed this line. We then calculated the response as the area under this curve. If the EOD rate did not recross the two s.d. line, the duration was calculated using the time of the minimum EOD rate between the start of the response and the end of the recording.

RESULTS

Knollenorgans are diverse in their frequency and duration tuning

We recorded KO spiking responses to constant-frequency sine waves (Fig. 1A,B). Stimuli above threshold elicited an increased number of spikes relative to the pre-stimulus period (Fig. 1A) whereas stimuli below threshold did not (Fig. 1B). Consistent with previous reports (Arnegard et al., 2006; Hopkins, 1981), all KOs were band-pass tuned, with BFs ranging from 0.35 to 4 kHz and BW_{10} values ranging from 0.30 to 9.69 kHz (Fig. 1C; Table 1). The range of peak power frequencies for *B. brachyistius* EODs was previously shown to range from 0.58 to 6.22 kHz (Fig. 1C) (Carlson et al., 2000).

We also recorded KO spiking responses to monophasic square pulses. Consistent with previous reports (Bennett, 1965; Hopkins and Bass, 1981), KOs generated a relatively fixed-latency spike in response to outside-positive edges of both positive and negative monophasic stimuli (Fig. 2A). This response was only observed when stimulus intensities were above threshold (Fig. 2B). All of the KOs were long-pass tuned for both stimulus polarities, with thresholds decreasing as duration increased (Fig. 2C). However, the shapes of these curves varied across KOs. We used an exponential fit to quantify variation in duration tuning (see Materials and methods). Values for a, which describes the asymptote of the fit, ranged from 0.01 to 0.96 nA and values for τ, which describes the time constant of the fit, ranged from 0.07 to 4.30 ms (Table 1). Total EOD duration in *B. brachyistius* was previously shown to range from 0.39 to 2.37 ms (Fig. 2C) (Carlson et al., 2000). For each KO, threshold range was calculated as the difference between the minimum and the maximum threshold over a given range of stimulus durations. Across the natural range of total EOD durations, the thresholds of individual KOs showed little variation (mean ± s.d. range of thresholds for stimulus durations between 0.39 and 2.37 ms=0.14±0.13 nA). However, the EODs of *B. brachyistius* consist of three distinct phases ranging in duration from 0.06 to 1.0 ms (Fig. 2C) (Carlson et al., 2000). These three phases are roughly similar to three monophasic square pulses in series. Therefore, EOD phase durations represent the behaviorally relevant range of stimulus durations when interpreting responses to monophasic square pulses. Across this range of durations, individual KO thresholds had four times the range of thresholds observed for the range of total EOD durations and eight times as much variation in the s.d. across KOs (mean range of thresholds ± s.d. for stimulus durations between 0.06 and 1.0 ms=0.61±1.10 nA). This difference was statistically

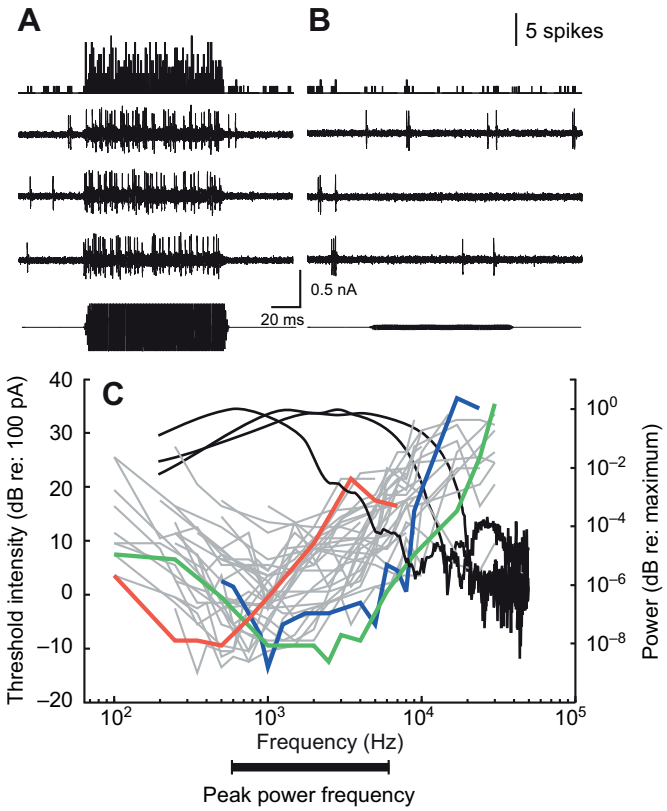

Fig. 1. Frequency tuning varies across knollenorgan electroreceptors. (A) Spike time histogram (top) and three selected traces (middle) from 15 repetitions of a 90 ms, 1 kHz, 0.63 nA stimulus (bottom) with 5 ms on and off ramps showing increased spike rate during the stimulus. (B) Spike time histogram (top) and three selected traces (middle) from 15 repetitions of a 90 ms, 1 kHz, 0.06 nA stimulus (bottom) with 5 ms on and off ramps illustrating a subthreshold response from the same knollenorgan. (C) Threshold frequency tuning curves from 32 different knollenorgans illustrating variability in frequency tuning. Three example knollenorgans, each from a different fish, are highlighted in red, blue and green, whereas all other knollenorgans are shown in gray. The fast Fourier transforms of the three sample electric organ discharges (EODs) illustrated in Fig. 2 are shown in black (sampling rate=100 kHz). The range of peak power frequencies (PPF) for *Brienomyrus brachyistius* EODs is shown below the threshold tuning curves (Carlson et al., 2000).

significant (paired t-test, t_{34}=2.49, P<0.02). Importantly, the diversity in KO tuning was not simply a result of diversity among fish, as different KOs from the same fish also varied in their tuning (Table 1, Fig. 3B).

Simple models reveal a link between frequency and duration tuning

To determine whether variation in duration tuning is related to variation in frequency tuning, we generated a simple electrical circuit model of KOs (Fig. 3A, inset; see Materials and methods). We adjusted both the capacitance and resistance values in this circuit to determine how changes in passive filtering properties affect frequency and duration tuning. First, with series resistance (R_s) and membrane resistance (R_m) held constant at 5 MΩ, increasing series capacitance (C_s) decreased the BF (Spearman rank r_S=–0.84, P<1e^{-6}) and the BW_{10} of frequency tuning curves (Spearman rank r_S=–0.78, P<1e^{-6}) of model KOs (Fig. 3A). Increasing C_s also increased the τ of the duration tuning curve (Spearman rank r_S=0.79, P<1e^{-6}) but did not have a significant effect on a (Spearman

Table 1. Knollenorgan diversity across and within fish

Fish ID	BF (Hz)	BW_{10} (Hz)	*a* (nA)	τ (ms)
BB0254	1000	4275	–	–
	1000	2609	0.3957	0.0885
	1500	2167	0.2707	0.2029
	2500	5842	0.7318	0.1111
BB0292	1000	3522	0.2225	0.2039
	1750	4825	0.4291	0.0742
BB0293	1500	7280	0.6803	0.0661
	–	–	0.3687	0.1161
BB0295	1000	539	–	–
	4000	8826	0.9603	0.0917
BB0296	1000	4817	–	–
	1000	632	0.1003	0.4876
	1000	9685	0.8469	0.6502
BB0297	500	946	0.0268	2.7843
	875	3310	0.0114	4.2978
	1000	6918	–	–
BB0298	500	300	–	–
	1000	1719	–	–
	1500	3330	0.3654	0.1272
BB0300	1000	1375	0.3014	0.1039
	–	–	0.3297	0.0909
BB0301	500	710	0.0947	0.5968
	1500	2788	0.3993	0.1587
	–	–	0.3209	0.1684
BB0302	350	1041	–	–
	1250	2677	0.2603	0.1284
BB0303	1200	1630	0.2010	0.5622
BB0304	350	445	0.1214	0.5215
	1000	972	0.1929	0.3230
BB0308	750	494	0.4167	0.1263
BB0376	750	1845	0.0887	0.2056
	750	1027	0.1073	0.4198
	1375	7036	0.2568	0.1509
	2500	4657	0.1415	0.1554
	3500	6897	0.2271	0.0321
	–	–	0.0331	2.0717

Frequency tuning is indicated by best frequency (BF) and bandwidth (BW_{10}). Duration tuning is summarized by *a*- and τ-values, as described in the Materials and methods.

rank r_S=–0.30, P=0.09). Increasing membrane capacitance (C_m) decreased both the BF and the BW_{10} of model KOs (Spearman rank r_S=–0.88, P<1e^{-6}, and r_S=–0.93, P<1e^{-6}, respectively) while increasing both *a* and τ (Spearman rank r_S=0.49, P<0.005, and r_S=0.96, P<1e^{-6}, respectively) of the duration tuning curve (Fig. 3A). With C_s and C_m held constant at 0.5 nF, increasing R_s non-significantly decreased BF and significantly decreased BW_{10} (Spearman rank r_S=–0.433, P=0.24, and r_S=–0.84, P<0.005, respectively) of model KOs while decreasing *a* and increasing τ of the duration tuning curve (Spearman rank r_S =–0.84, P<0.005, and r_S=0.84, P<0.005, respectively; Fig. 3A). Increasing R_m did not lead to any significant changes in BF, BW_{10}, *a* or τ (Spearman rank r_S=–0.43, P=0.24; r_S=–0.47, P=0.20; r_S=–0.47, P=0.2; r_S=0.47, P=0.2, respectively).

As a result of these effects, there was a strong negative correlation between BF and τ among our model KOs (Spearman rank r_S=–0.90, P<1e^{-6}), as well as between BW_{10} and τ (Spearman rank r_S=–0.99, P<1e^{-10}). Neither BF nor BW_{10} were significantly correlated with *a* (Spearman rank r_S=–0.18, P>0.3, and r_S=–0.22, P>0.2, respectively). The three sample tuning curves shown in Fig. 3A illustrate the relationship between frequency and duration tuning of model KOs, but it is important to realize that these particular combinations of capacitance and resistance do not necessarily represent a unique solution for those particular tuning curves. Similar correlations between frequency and duration tuning were observed among different KOs recorded from a single fish (Fig. 3B). Indeed, across all KOs, BF and BW_{10} were negatively correlated with τ (Spearman rank r_S=–0.67, P<1e^{-3} and r_S=–0.46, P<0.03, respectively).

Stronger signals create tighter responses

The accuracy of temporal coding depends on the precision of time-locked responses to stimuli. However, temporal precision in sensory systems is generally intensity dependent. Therefore, we investigated how stimulus intensity affected the timing of KO responses. Decreasing stimulus intensity led to a consistent increase in response

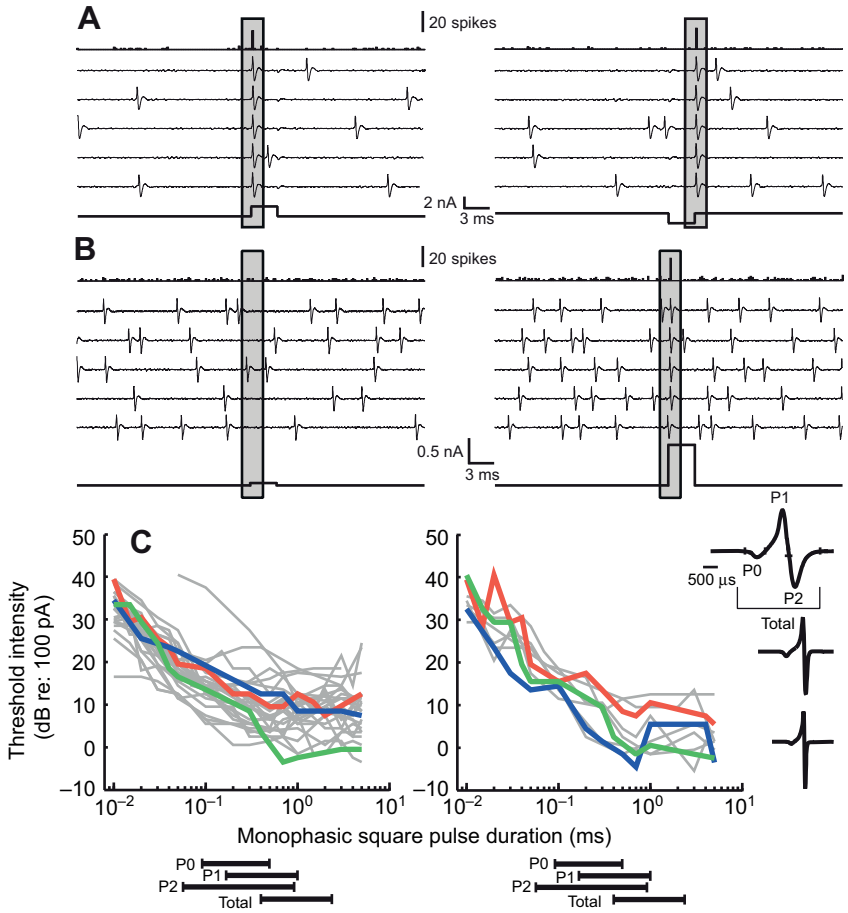

Fig. 2. Duration tuning varies across knollenorgan electroreceptors. (A) Spike time histograms (top) and five selected traces (middle) from 25 repetitions of a 2 nA, 3 ms square pulse (bottom) showing a time-locked spike to the upward edge of both monophasic positive (left) and negative (right) stimuli from the same knollenorgan. (B) Spike time histograms (top) and five selected traces (middle) from 25 repetitions of a 0.08 nA (left) and 0.8 nA (right), 3 ms square pulse (bottom) illustrating the difference between a subthreshold (left) and suprathreshold (right) response from a second knollenorgan. (C) Threshold tuning curves in response to normal (left; *N*=27) and reverse (right; *N*=9) polarity square pulses illustrate the diversity of duration tuning across knollenorgans. Tuning curves from three knollenorgans, each from a different fish, are highlighted in red, blue and green; all other knollenorgans are shown in gray. For each knollenorgan, the tuning curves in response to positive and negative polarity stimuli are shown in the same color. Three sample EODs are shown to the right (sampling rate=100 kHz), and the three distinct phases (P0, P1 and P2) are illustrated in the topmost EOD. The range of durations for each phase of the EOD and the total EOD durations of *B. brachyistius* are shown below (Carlson et al., 2000).

latency (i.e. amplitude-dependent latency shift), as well as an increase in the variability of response times (i.e. jitter; Fig. 4A). This effect was consistent across the five KOs tested with a range of stimulus durations (Fig. 4B–D). Mean first spike latency decreased significantly with increasing stimulus intensity in all cases (range of Spearman rank r_S=–1 to –0.85, P<0.05; Fig. 4B). First spike latency s.d. also decreased significantly with increasing stimulus intensity in 11 of the 12 cases (range of Spearman rank r_S=–0.92 to –0.62, P<0.05; Fig. 4C). Finally, relative response probability increased significantly with increasing stimulus intensity in all cases (range of Spearman rank r_S=0.60 to 0.97, P<0.05; Fig. 4D). Therefore, the temporal precision needed for accurately coding stimulus duration into spike latency differences was greatest at relatively high intensities.

Midbrain responses reflect the peripheral coding of duration

We next asked how the diversity of duration coding by KOs influenced electrosensory responses within the central KO pathway. We recorded evoked field potentials in ELa and ELp in response to monophasic and biphasic square pulses presented at an intensity of 3.7 mV cm^{-1} and varying in total duration from 0.01 to 20 ms. Normalized responses, measured as the total area of the evoked potential, increased with increasing duration for both monophasic (Fig. 5A, top panel) and biphasic square pulses (Fig. 5B, top panel). Using a repeated-measures ANOVA, we found a significant increase in normalized responses with increasing duration for monophasic ($F_{13,143}$=51.8, P<1e^{-6}) and biphasic pulses ($F_{13,117}$=34.7, P<1e^{-6}). In comparing isointensity tuning curves for ELa and ELp, there was no significant interaction effect between recording location and stimulus duration for monophasic ($F_{13,143}$=0.6, P>0.84) or biphasic stimuli ($F_{13,117}$=1.2, P>0.27), indicating no difference in the isointensity duration tuning curves of evoked potential responses of the two midbrain regions.

We also measured threshold stimulus intensities for evoked field potentials in ELa and ELp in response to monophasic and biphasic square pulses with total durations ranging from 0.01 to 20 ms. For both monophasic (Fig. 5A, middle panel) and biphasic (Fig. 5B, middle panel) square pulses, we found greater sensitivity to longer pulse durations in both ELa and ELp (repeated-measures ANOVA, monophasic $F_{16,96}$=27.0, P<1e^{-6}; biphasic $F_{11,99}$=37.6, P<1e^{-6}). There was no significant interaction effect between recording location and stimulus duration for either monophasic ($F_{16,96}$=0.5, P>0.95) or biphasic stimuli ($F_{11,99}$=0.7, P>0.75), indicating that there was no difference in the threshold duration tuning curves of evoked potential responses of the two midbrain regions. Importantly, the range of durations over which ELa and ELp showed the greatest change in both isointensity response and threshold intensity directly corresponded to the range of durations over which KOs exhibited the greatest variation in threshold (compare Fig. 5 with Fig. 2C). This suggests that the long-pass tuning observed in ELa and ELp was due to the progressive recruitment of additional KOs with increasing stimulus duration.

To ensure that long-pass tuning was consistent across a range of intensities, we measured the magnitude of evoked potentials in response to intensities ranging from 0.11 to 35.4 mV cm^{-1}. In ELa, we observed long-pass tuning at all intensities ≥1.1 mV cm^{-1}, and these curves did not saturate even at the longest durations and intensities tested (supplementary material Fig. S1A). In ELp, we also

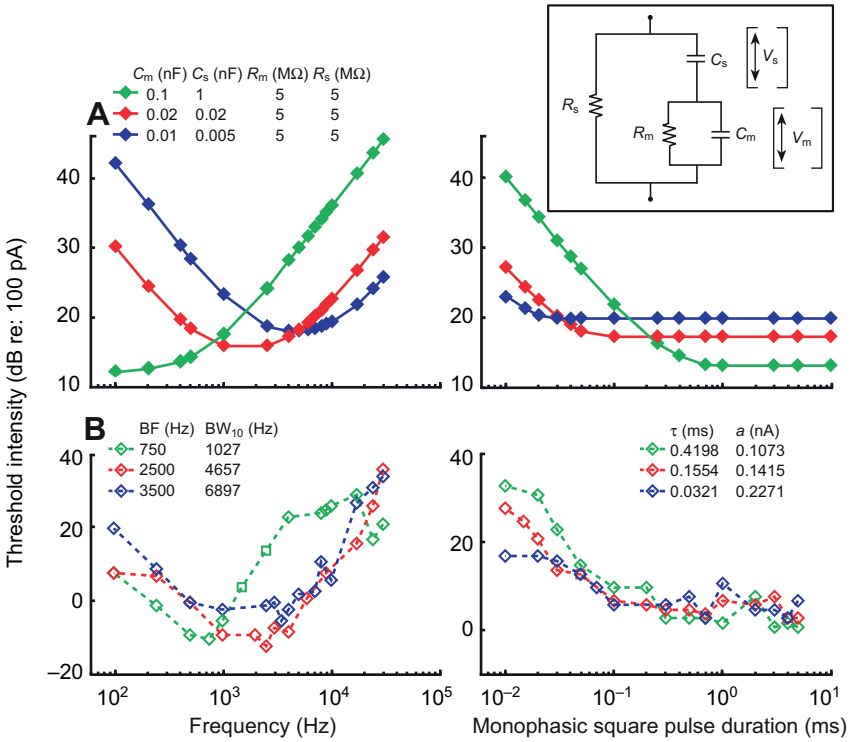

Fig. 3. Modeling the knollenorgan receptor as a simple electrical circuit. (A) Frequency (left) and duration (right) tuning curves generated from three model neurons with resistance values set to 5 MΩ and variable capacitance values as indicated. Inset shows the electrical circuit model of knollenorgan receptors, which consists of skin resistance (R_s), membrane resistance (R_m), membrane capacitance (C_m) and series capacitance (C_s). Corresponding voltage drops (V_s and V_m) across the two capacitors are shown with arrows. (B) Frequency (left) and duration (right) tuning curves from three different knollenorgans recorded from a single fish with measured values for best frequency (BF), bandwidth (BW_{10}), duration tuning curve time constant (τ) and duration tuning curve asymptote (*a*).

observed long-pass tuning at all intensities ≥1.1 mV cm^{-1}, although the curve saturated at ~0.1 ms at the higher intensities tested (supplementary material Fig. S1B).

Increasing the duration of a square pulse increases the total energy of the stimulus. To determine whether the observed long-pass tuning was due solely to the effects of increasing stimulus energy, we determined the threshold energy (threshold intensity multiplied by duration) as a function of duration. If changes in energy fully accounted for the observed long-pass tuning, then we would expect threshold energy to be the same for all durations; however, threshold energy increased with duration for both monophasic ($F_{16,96}$=23.3, P<1e^{-6}; Fig. 5A, bottom panel) and biphasic stimuli ($F_{11,99}$=57.1, P<1e^{-6}; Fig. 5B, bottom panel).

Behavioral responses reflect the peripheral coding of duration

Next, we determined how the diversity of duration coding by KOs impacted behavioral responses to electrosensory stimulation. To assess this, we used the 'novelty response', which is an increase in the rate of EOD emission in response to the presentation of a novel stimulus (Carlson et al., 2011; Post and von der Emde, 1999). We presented monophasic and biphasic square pulses ranging in duration from 0.01 to 10 ms at an intensity of 145 mV cm^{-1}. We measured EOD frequency over time by convolving EOD times of occurrence with a 300-ms-wide Gaussian function (Carlson and Hopkins, 2004) and averaging across repetitions. The magnitude of the novelty response was calculated as the area under the response curve (Fig. 6A; see Materials and methods). The magnitude of the fish's response increased with stimulus duration for both monophasic (repeated-measures ANOVA, $F_{13,117}$=6.9, P<1e^{-6}; Fig. 6B, top panel) and biphasic stimuli ($F_{13,104}$=3.2, P<1e^{-3}; Fig. 6D, top panel). The threshold intensity necessary to elicit a novelty response decreased with stimulus duration for both monophasic ($F_{10,40}$=4.8, P<1e^{-3}; Fig. 6B, middle panel) and biphasic stimuli ($F_{10,50}$=4.8, P<1e^{-4}; Fig. 6D, middle panel). Finally, we tested whether stimulus energy was the sole source of long-pass tuning by plotting threshold energy against stimulus duration. As with evoked potentials in ELa and ELp, threshold energy increased with increasing stimulus duration for both monophasic ($F_{10,40}$=2.5, P<0.021; Fig. 6B, bottom panel) and biphasic stimuli ($F_{10,50}$=4.9, P<1e^{-4}; Fig. 6D, bottom panel). To determine whether stimulus intensity impacted the shape of the isointensity tuning curve, we measured the magnitude of the responses of one fish for 0.01 to 10 ms monophasic pulses presented at seven intensities ranging from 14 to 725 mV cm^{-1} and observed long-pass tuning at each intensity (Fig. 6C).

Peripheral coding of duration affects detection of natural stimulus waveforms

Finally, we tested how the coding of duration by KOs affected the detection of behaviorally relevant stimuli by measuring KO threshold intensities to natural EOD waveforms of 10 different mormyrid species. We also measured thresholds to *B. brachyistius* EODs subjected to three different temporal manipulations: cutting the duration in half, doubling the duration and time-reversing the EOD.

KOs responded to the rising edge of a natural waveform with a fixed-latency spike (Fig. 7A), just as they did to square pulses (Fig. 2A,B). KO threshold intensity varied in response to different species' EODs (repeated-measures ANOVA, $F_{11,88}$=10.5, P<1e^{-6}; Fig. 7B), but there was no difference in threshold between normal and reversed polarities ($F_{1,8}$=2.2, P>0.1). The peak power frequencies (PPFs) of EODs negatively correlate with duration (Hopkins, 1981). We therefore used PPF to quantify species differences in EOD waveforms, and found that KO thresholds decreased significantly with decreasing PPF (Spearman rank r_S=0.62, P<0.05). We presented waveforms recorded from three different *B. brachyistius* individuals and found mean thresholds of 3.34±0.84, 3.50±0.70 and 3.10±0.34 nA for normal polarity stimuli and 2.26±0.48, 2.87±0.62 and 1.96±0.39 nA for reverse polarity stimuli. The thresholds for the three waveforms were not significantly different from each other ($F_{2,20}$=1.8, P>0.1), nor were the thresholds of normal *versus* reversed polarity stimuli ($F_{1,10}$=2.3, P>0.1).

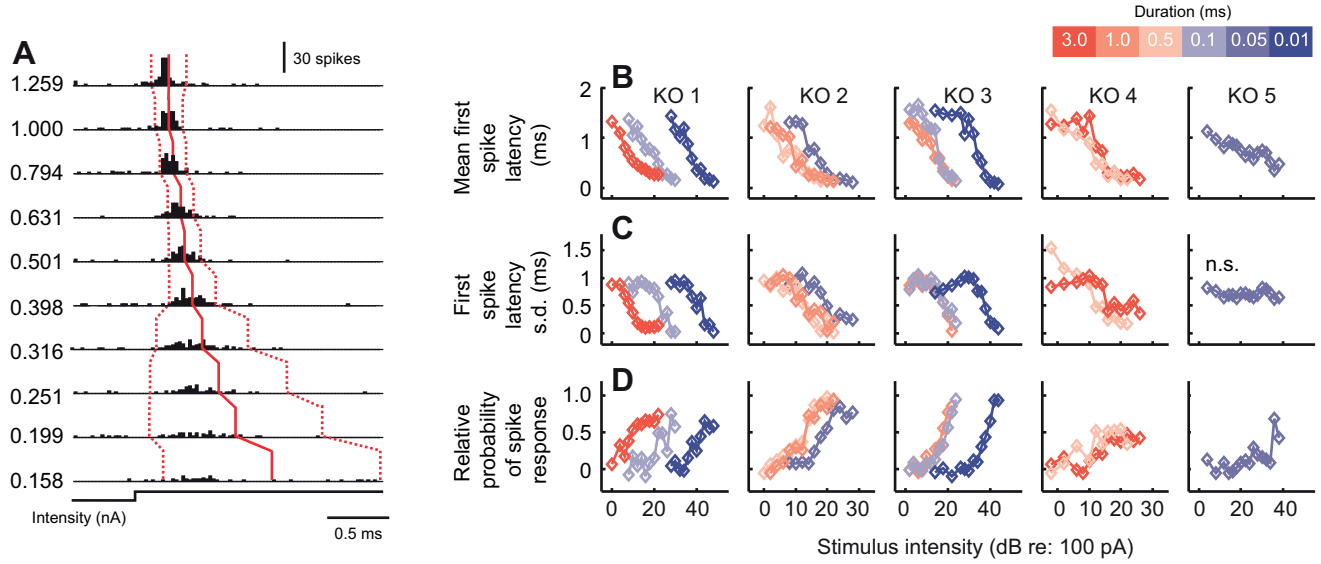

Fig. 4. Knollenorgan spike latency and variability is stimulus intensity dependent. (A) Spike time histograms from a single knollenorgan in response to 100 repetitions of a 3 ms monophasic positive square pulse stimulus presented at intensities ranging from 0.158 to 1.259 nA. Mean and s.d. of first spike latencies are shown as solid and dashed red lines, respectively. (B–D) Responses to six different durations tested twice each across five knollenorgans for a total of 12 experiments. (B) Mean first spike latency decreases with increasing stimulus intensity (Spearman rank r_S=–1 to –0.85, P<0.05). (C) Standard deviation of first spike latency decreases with increasing stimulus intensity (Spearman rank r_S=–0.92 to –0.62, P<0.05). n.s., the correlation between the response measure and stimulus intensity was not significant. (D) Relative probability of spike response, calculated as the number of spikes per stimulus relative to pre-stimulus baseline activity (see Materials and methods), increases with increasing stimulus intensity (Spearman rank r_S=0.6 to 0.97, P<0.05).

Artificial manipulation of the duration of a *B. brachyistius* EOD caused a significant change in KO threshold (repeated-measures ANOVA, $F_{2,22}$=22.0, P<1e^{-5}), with lower thresholds for elongated EODs and higher thresholds for shortened EODs. There was no difference between normal and reverse polarity stimuli ($F_{1,11}$=0.63, P>0.4). For the time-reversed EOD, neither the normal (t_6=0.59, P>0.5) nor the reverse polarity thresholds (t_4=–0.02, P>0.95) were significantly different from the natural EOD (Fig. 7B).

The magnitude of evoked potentials in ELp also differed significantly in response to different species' EODs (repeated-measures ANOVA, $F_{11,66}$=11.3, P<1e^{-6}; Fig. 7C). Evoked potentials increased significantly in magnitude with decreasing PPF (Spearman rank r_S=–0.61, P<0.05). Artificial manipulation of the duration of a *B. brachyistius* EOD significantly changed the magnitude of evoked potential responses ($F_{2,22}$=11.0, P<1e^{-3}), with larger responses to elongated EODs and weaker responses to shortened EODs. Unlike at the periphery, the time-reversed waveform evoked a significantly smaller response (t_{12}=–2.3, P<0.05; Fig. 7C).

Finally, behavioral measures of sensitivity also showed duration dependence. Normalized behavioral responses did not differ significantly in response to different species' EODs, although there was a clear trend (repeated-measures ANOVA, $F_{11,55}$=1.8, P<0.1), but behavioral thresholds did differ significantly in response to different species' EODs ($F_{11,66}$=7.4, P<1e^{-6}). Further, normalized behavioral responses increased significantly with decreasing PPF (Spearman rank r_S=–0.88, P<0.05; Fig. 7D), and behavioral thresholds decreased significantly with decreasing PPF (Spearman rank r_S=0.94, P<0.05; Fig. 7E). Neither behavioral threshold ($F_{2,12}$=0.3, P>0.7) nor normalized behavioral responses ($F_{2,12}$=0.2, P>0.8) differed significantly in response to artificial manipulation of EOD duration. Similarly, the time-reversed waveform was not significantly different from the original waveform for either normalized behavioral responses (t_6=1.4, P>0.2) or behavioral thresholds (t_6=0.3, P>0.7; Fig. 7D,E).

DISCUSSION

We asked how variation among peripheral sensory receptors impacts the coding of stimulus duration. We found that KO electroreceptors exhibit variable long-pass duration tuning (Fig. 2C). The diversity in duration tuning correlates with variation in frequency tuning, as predicted by a simple circuit model of KOs (Fig. 3). Population responses in two midbrain nuclei that process electrosensory communication signals are also long-pass tuned to duration (Fig. 5), as are behavioral novelty responses (Fig. 6). Importantly, both midbrain and behavioral thresholds varied most dramatically across the same range of durations for which KO receptors exhibited the greatest diversity in tuning. This window of stimulus durations corresponds to the range of durations observed for different phases of conspecific EODs (Carlson et al., 2000). In relating natural EODs to monophasic square pulses, we propose that the range of EOD phase durations, not the range of total EOD durations, represents the behaviorally relevant range of stimulus duration. The triphasic EOD of *B. brachyistius* is roughly similar to three monophasic square pulses in series. KO receptors respond to either rising or falling edges, which occur at the start or end of each phase of a natural EOD and at the start or end of a monophasic square pulse. Indeed, responses to natural waveforms from a variety of species that vary widely in EOD duration demonstrate duration-dependent differences in sensitivity, confirming the relevance of peripheral duration tuning to the detection and discrimination of natural signals (Fig. 7).

Peripheral diversity creates a population code for duration

Multiple observations on the response properties of KOs (Bennett, 1965; Bell, 1990; Zakon, 1986) led Hopkins and Bass (Hopkins and Bass, 1981) to propose a temporal coding model for species recognition, in which EOD duration is coded by spike timing differences between KOs on opposite sides of the body (Fig. 8). Several lines of evidence suggest that these differences in spike timing are compared within the ELa to establish single-neuron tuning to

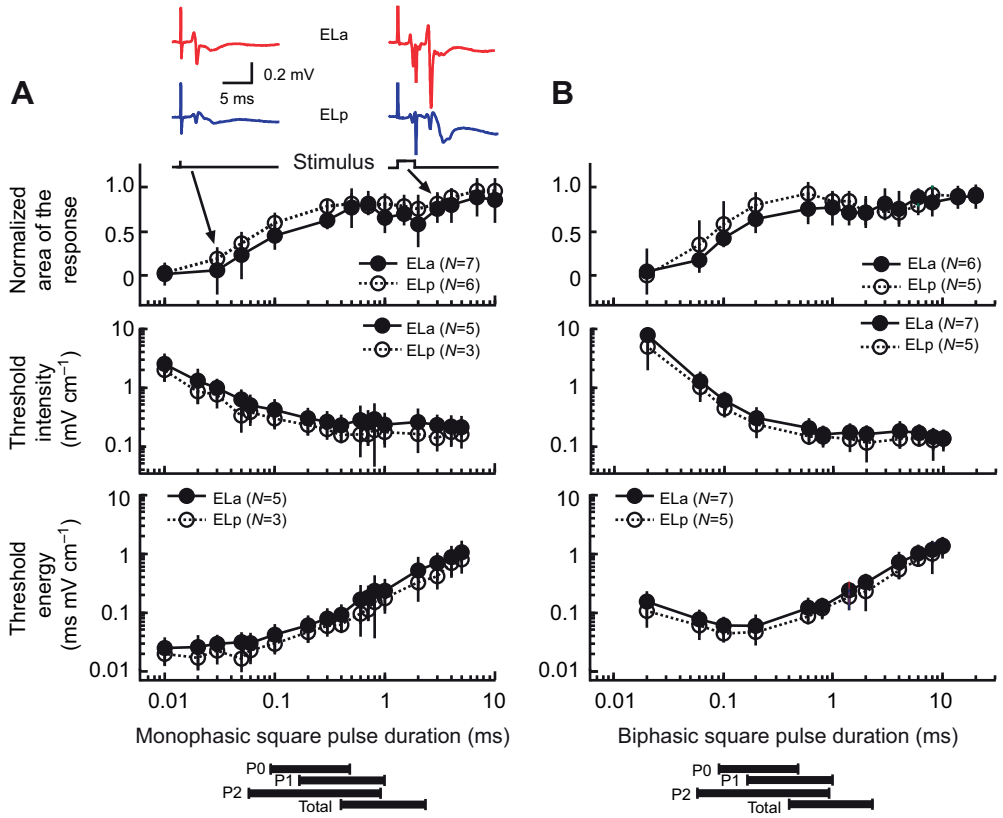

Fig. 5. Duration tuning of evoked potentials in the exterolateral nucleus (EL) of the midbrain reveals changes in sensitivity across the range of natural EOD durations. Mean isointensity tuning curves in response to monophasic (A, top) and biphasic (B, top) square pulses of varying durations in both the anterior (filled circles) and posterior (open circles) subdivisions of the EL (ELa and ELp, respectively). Example evoked potential responses from the ELa (red) and the ELp (blue) at two different stimulus durations (arrows) are shown. Each region has a unique, characteristic response shape. Therefore, responses were normalized to the largest response across all durations tested for the same nucleus in the same fish. Normalized responses increase with increasing stimulus duration for both monophasic ($F_{13,143}$=51.8, P<1e^{-6}) and biphasic ($F_{13,117}$=34.7, P<1e^{-6}) pulses. Isointensity tuning curves were generated with a stimulus intensity of 3.7 mV cm^{-1}, and all response magnitudes were normalized to the largest response for each fish. Threshold intensity tuning curves in response to monophasic (A, middle) and biphasic (B, middle) square pulses of varying durations in both brain regions decrease with increasing stimulus duration for both monophasic ($F_{16,96}$=27.0, P<1e^{-6}) and biphasic ($F_{11,99}$=37.6, P<1e^{-6}) pulses. Threshold energy tuning curves in response to monophasic (A, bottom) and biphasic (B, bottom) square pulses of varying durations in both brain regions increase with increasing stimulus duration (monophasic, $F_{16,96}$=23.3, P<1e^{-6}; biphasic, $F_{11,99}$=57.1, P<1e^{-6}). Values shown are the means ± s.d. across fish. The range of durations for each phase of the EOD (P0, P1 and P2) and the total EOD durations of *B. brachyistius* are shown below (Carlson et al., 2000).

stimulus duration (Amagai, 1998; Amagai et al., 1998; Friedman and Hopkins, 1998; Carr and Friedman, 1999; Mugnaini and Maler, 1987; Xu-Friedman and Hopkins, 1999). However, as stimulus intensity decreased, we found significant decreases in KO response probability and significant increases in response latency and jitter (Fig. 4), revealing that the temporal coding of stimulus duration is less effective at near-threshold intensities. Sound intensity similarly affects the accuracy of temporal coding for sound localization (Nishino et al., 2008). Population averaging of peripheral responses through anatomical convergence is one mechanism for reducing temporal jitter in auditory and electrosensory systems (Carr and Friedman, 1999). Our data suggest another solution to this problem: a population code allows fish to obtain information about stimulus duration at intensities too low for a temporal code to reliably signal duration. Using our particular behavioral measure (the novelty response), threshold detection levels for natural EOD waveforms ranged from 0.06 to 0.74 mV cm^{-1} (Fig. 7E). Work in other mormyrid species based on more sensitive measures of signal detection has revealed a minimum threshold for detection of communication signals as low as 1–10 μV cm^{-1} (Moller and Bauer, 1973; Moller et al., 1989). Paintner and Kramer (Paintner and Kramer, 2003) demonstrated that the minimum intensity for trained mormyrids to discriminate a 2 μs difference in waveform ranged from 4.9 to 123 μV cm^{-1}. Using evoked potential responses in ELa and ELp as a readout of the KO population response, we found that threshold intensities to monophasic square pulses ranged from 140 μV cm^{-1} to 2.54 mV cm^{-1} (Fig. 5A). Therefore, stimulus intensities greater than 2.5 mV cm^{-1} are necessary for all KOs to respond reliably and this value is well above the minimum intensity for accurate signal discrimination. Even restricting the range of durations to the behaviorally relevant phase durations of 0.06 to 1 ms, we found that threshold intensities ranged from 176 to 508 μV cm^{-1} (Fig. 5A). Therefore, mormyrids can discriminate species-specific EODs at intensities that are too weak for the temporal code to work effectively.

Each KO studied exhibited long-pass tuning (Fig. 2C), as expected because of membrane capacitance, which acts as a low-pass filter of input current for all neurons. Interestingly, however, long-pass tuning characteristics differed among KOs, both between and within fish, over the range of behaviorally relevant durations corresponding to the range of EOD phase durations (Fig. 2C, Fig. 3B, Table 1). Therefore, at near-threshold intensities, increasing stimulus duration across the behaviorally relevant range leads to the recruitment of an

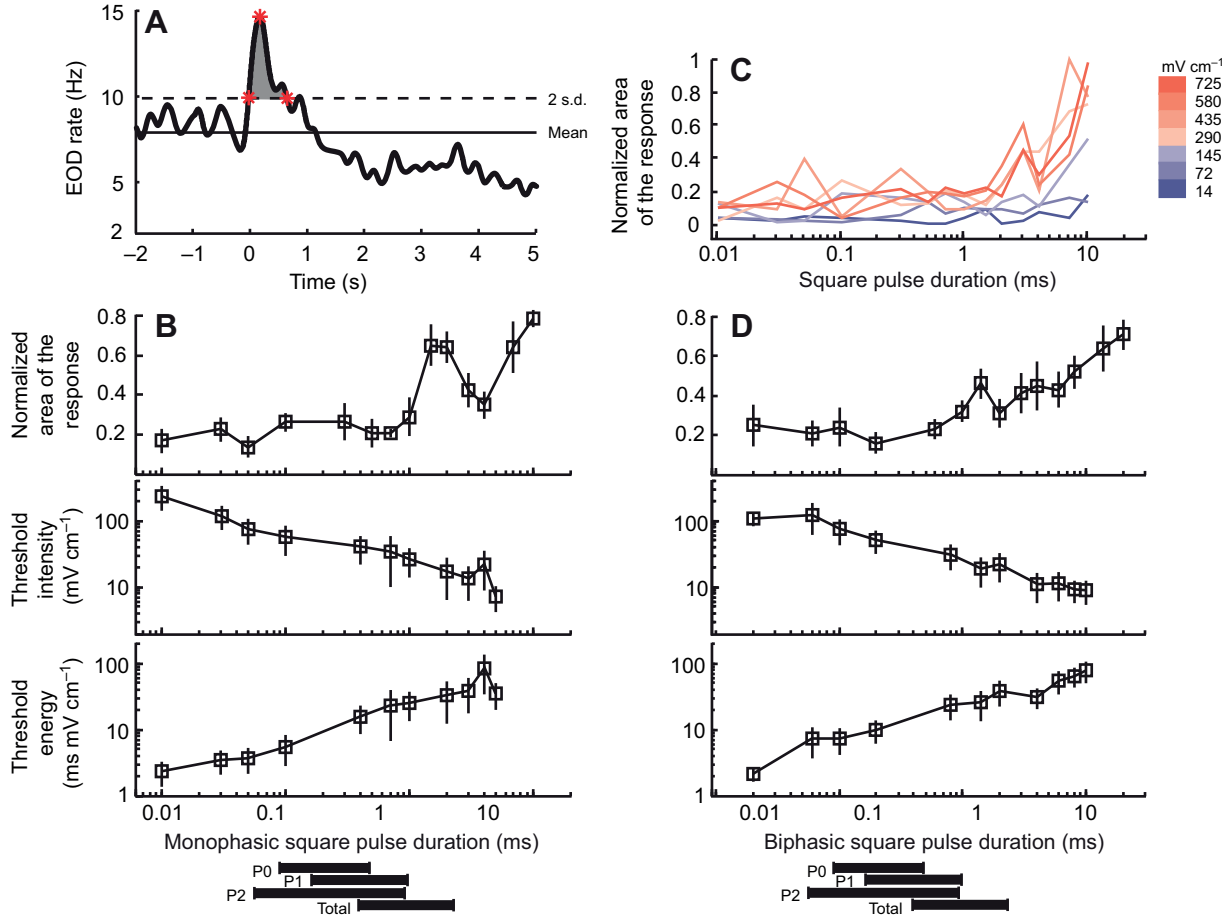

Fig. 6. Duration tuning of behavioral novelty responses reveals changes in sensitivity across the range of natural EOD durations. (A) Example of increased EOD rate (novelty response) in response to a biphasic square pulse delivered at time=0 s. Isointensity responses were calculated using the area under the curve above the two s.d. line (gray fill). (B) Normalized response ($F_{13,117}$=6.9, P<1e^{-6}, N=10; top), threshold intensity ($F_{10,40}$=4.8, P<1e^{-3}, N=5; middle) and threshold energy ($F_{10,40}$=2.5, P<0.021, N=5; bottom) tuning curves for novelty responses to monophasic square pulses of varying durations. (C) Isointensity tuning curves for monophasic square pulses presented at a range of intensities (14 to 725 mV cm^{-1}) all show long-pass tuning (N=1). (D) Normalized response ($F_{13,104}$=3.2, P<1e^{-3}, N=9; top), threshold intensity ($F_{10,50}$=4.8, P<1e^{-4}, N=6; middle) and threshold energy ($F_{10,50}$=4.9, P<1e^{-4}, N=6; bottom) tuning curves for novelty responses to biphasic square pulses of varying durations. Values shown are means ± s.d. The range of durations for each phase of the EOD (P0, P1 and P2) and the total EOD durations of *B. brachyistius* are shown below (Carlson et al., 2000).

increasing number of KOs (Fig. 8). As increases in both stimulus intensity and duration will lead to the recruitment of more KOs (Fig. 8), there is some ambiguity to a simple population code based solely on the number of responding receptors. Importantly, we found that the shape of each KO's tuning curve differs (Fig. 2C, Fig. 3B, Table 1), meaning that different combinations of stimulus duration and intensity will result in unique patterns of population-level responses (Fig. 8).

Two codes for stimulus duration, one circuit

Together, these observations suggest two distinct mechanisms for the peripheral coding of stimulus duration (Fig. 8). At relatively high stimulus intensities (i.e. >1 nA; see Fig. 2C), all KOs are above threshold across the behaviorally relevant range of durations, so a temporal code based on spike latency differences would allow for reliable coding of stimulus duration. However, at near-threshold intensities (i.e. 0.1–1 nA; see Fig. 2C), for which a temporal code is less effective, increasing stimulus duration leads to the recruitment of an increasing number of KOs, suggesting a population code for stimulus duration. Although it is unclear how a given amount of current injected directly into a receptor organ corresponds to the amount of current that would result from a natural electric field, the two will scale linearly. Thus, our results make it clear that there is a 10-fold range of stimulus intensities just above threshold over which stimulus duration is represented by both the number and the identity of responding KOs (Fig. 2C).

Based on anatomical evidence, Friedman and Hopkins (Friedman and Hopkins, 1998) proposed a delay-line anti-coincidence detection model for the recoding of peripheral spike latency differences. According to this model, small cells in the ELa receive delayed excitation from one receptive field, and inhibition from local interneurons (Mugnaini and Maler, 1987; George et al., 2011) corresponding to a different receptive field. As a result, small cells only respond when a stimulus is long enough such that onset-triggered delayed excitation arrives before offset-triggered inhibition, resulting in long-pass tuning to stimulus duration. Differences in excitatory delay would establish variation in the minimum stimulus duration needed to elicit a response across the population of small cells. As a result, increases in stimulus duration would increase small cell recruitment, thereby recoding the peripheral temporal code into a population code for duration (Xu-Friedman and Hopkins, 1999).

By identifying a potential mechanism for converting a temporal code into a population code, the Friedman–Hopkins model reveals

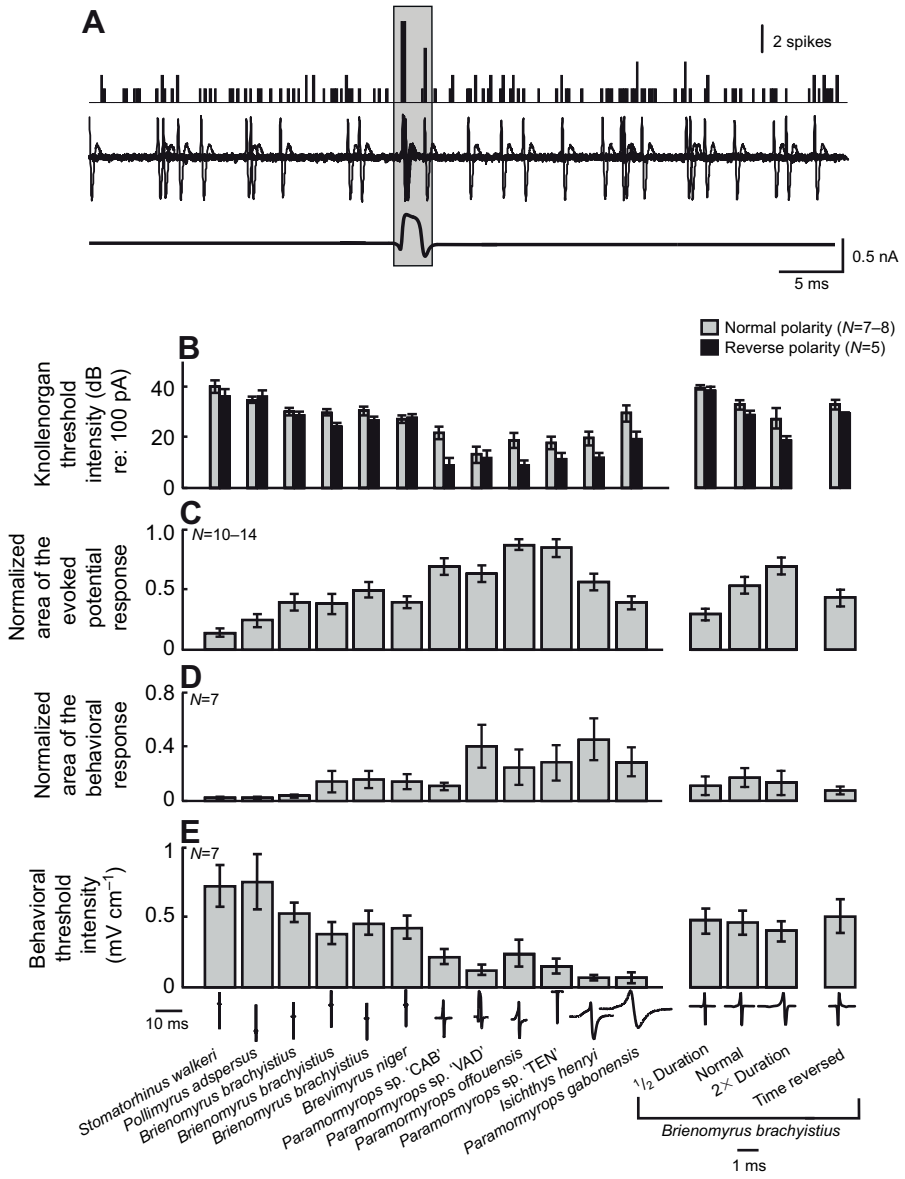

Fig. 7. Sensitivity to natural and manipulated EOD waveforms is duration dependent. (A) Spike time histogram (top) and five superimposed selected traces from 25 repetitions of a *Paramormyops vadamans* EOD presented at 0.63 nA showing a time-locked knollenorgan spike to the upward edge. (B) Knollenorgan response thresholds to EOD waveforms from 10 different species vary significantly (left), as do manipulated versions of *B. brachyistius* EODs (right). (C) Normalized ELp mean evoked potential responses to the same waveforms from B. Normalized behavioral (D) and threshold (E) responses to the same waveforms from B. Waveforms and species names are shown below each column of data, which are arranged in order of decreasing peak power frequency. Three-letter cheironyms refer to undescribed species of *Paramormyrops* recently discovered in Gabon, Africa (Arnegard et al., 2005; Arnegard and Hopkins, 2003; Carlson et al., 2011; Sullivan et al., 2002). Values shown are means ± s.e.m.

how the peripheral code for stimulus duration at high stimulus intensities can be converted into the same type of code we found to operate at low intensities, potentially establishing a single common population code among small cells for all intensities. Evoked potentials in both the ELa and the ELp scale with stimulus duration across a wide range of intensities (supplementary material Fig. S1), consistent with a small cell population code for stimulus duration. However, multiple different intensity/duration combinations elicit the same evoked potential response (supplementary material Fig. S1). As evoked potentials reflect the summed activity of populations of neurons, this overlap indicates that a population code based simply on the number of active small cells would not unambiguously code for stimulus duration. As with the population coding of stimulus duration by KO receptors, we propose that stimulus duration may be represented by unique spatial patterns of responsive small cells. This type of population-coding scheme could also allow for the coding of other behaviorally relevant attributes of EODs, such as intensity, orientation and polarity. Neurons in ELp exhibit tuning to all of these stimulus attributes (Amagai, 1998), as well as to the interpulse intervals between EODs (Carlson, 2009), so this information is clearly encoded in the output of small cells.

If a population code can be used to obtain information about stimulus duration, then why would there also be a temporal code, which is associated with anatomical features that are presumably energetically expensive, such as large cells, thick axons and heavy myelination (Carr and Friedman, 1999)? It is likely that a 'start-stop' peripheral code provides for greater temporal precision, whereas a peripheral population code would still provide some information about duration at low intensities that do not allow for this level of precision. Further, a key aspect of a temporal code for stimulus duration is that it greatly extends the dynamic range of the system. A population code for duration is intensity dependent: above a certain intensity, the system will saturate (all receptors will respond to all durations) and information about stimulus duration cannot be encoded into changes in the population of responding receptors. By contrast, a 'start-stop' temporal code never saturates (Bennett, 1965; Hopkins and Bass, 1981).

Differences in passive and active membrane properties may explain peripheral variation

Previous studies have shown that KOs are band-pass tuned to frequencies close to the peak power frequencies of conspecific EODs (Arnegard et al., 2006; Bass and Hopkins, 1984; Hopkins, 1981).

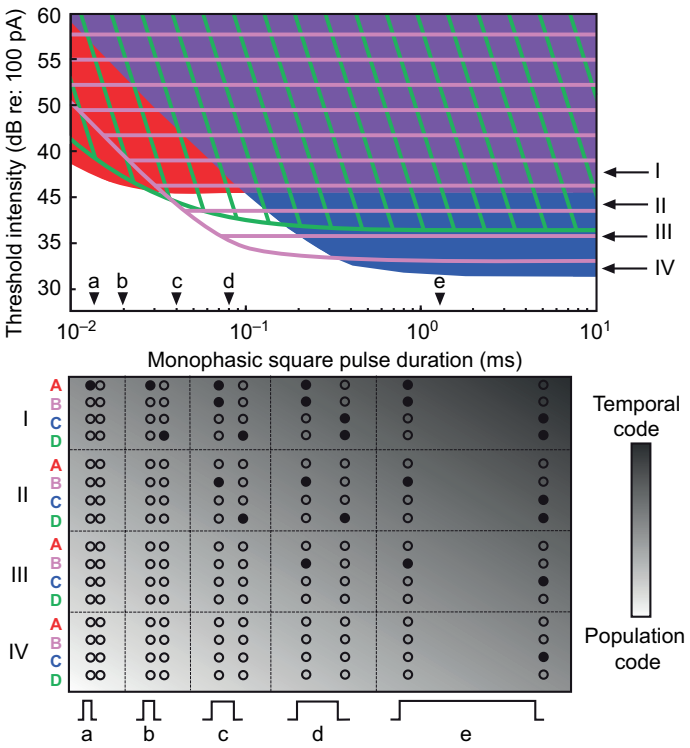

Fig. 8. Conceptual model of duration tuning utilizing a temporal code at high intensities and a population code at low intensities. In the top plot, threshold duration tuning curves from four model knollenorgans are shown with shading to indicate suprathreshold response regions. The different colors indicate the duration and intensity combinations that will elicit a response from each model knollenorgan (knollenorgan A=red, knollenorgan B=pink, knollenorgan C=blue, knollenorgan D=green). Example responses of the same four model knollenorgans to stimuli at four different intensities (arrows) and five different durations (arrowheads) are shown in the plot below. Filled circles indicate a response, whereas open circles indicate a lack of response, with background shading indicating the transition between a temporal code and a population code. At high intensities and long durations, spike timing differences between knollenorgans responding to the start of the pulse (A,B) and knollenorgans responding to the end of the pulse (C,D) provide a precise temporal code for duration. In contrast, shorter and weaker stimuli are characterized by a population code in which duration is represented by the number and identity of responsive knollenorgans (filled circles).

We confirmed this (Fig. 1C), finding variation in the range of best frequencies and bandwidths both between and within fish (Fig. 3B, Table 1). Variability in frequency tuning among the population of receptors is indicative of physiological differences that should also affect duration tuning. Indeed, we found that the duration- and frequency-tuning characteristics of KOs were correlated in the same way as simple models in which we systematically varied membrane and series capacitances and resistances (Fig. 3). Thus, differences in capacitance or resistance between KOs could account for the observed covariation in frequency and duration tuning. Ampullary receptors could potentially contribute to behavioral responses because they respond to the DC components of monophasic square pulses (Bennett, 1965; Zakon, 1986). However, biphasic pulses do not have a DC component, and behavioral responses to monophasic and biphasic square pulses were similar (Fig. 6). Further, ELa and ELp do not receive input from the ampullary system (Bell and Szabo, 1986), and the responses of these nuclei were consistent with the behavioral results (Figs 5, 6).

Variation in capacitive or resistive properties could result from differences in electroreceptor organ morphology (Zakon, 1986). KOs are tuberous electroreceptors composed of a canal leading to a sensory chamber typically containing one to 10 sensory cells, each 40–50 µm in diameter (Bennett, 1965; Szabo, 1965; Harder, 1968b; Zakon, 1986). The canal is lined by a wall composed of numerous layers of flattened epithelial cells and it is filled with a plug of loosely packed epithelial cells (Szabo, 1965). The epithelial plug, which is not present in low-frequency ampullary electroreceptors, establishes a series capacitance (Fig. 3A, inset) that acts as a high-pass filter of current through the organ (Zakon, 1986). Differences in the number of cells within the epithelial plug or in their morphology could establish variation in series capacitance. The canal walls of tuberous electroreceptors may also contribute to the series capacitance of receptors (Zakon, 1986). Tuberous receptors in gymnotiforms have more layers of flattened epithelial cells in the canal wall than ampullary receptors, suggesting that differences in tuning between the two receptor types relates to differences in the capacitive contribution of the canal wall (Bennett, 1971). Indeed, the maximum number of layers within the capsular wall of tuberous organs varies from 10 to 60 across nine different species of gymnotiform fishes, and this variation correlates with receptor frequency tuning (Lissmann and Mullinger, 1968; Zakon, 1986). There is even extensive variation in tuberous organ morphology within species: among tuberous receptors of the gymnotiform *Hypopomus*, the number of layers of flattened epithelial cells varies from 10 to 50, causing the wall thickness to vary from 2 to 5 µm (Szamier and Wachtel, 1970). In mormyrids, Harder (Harder, 1968b) reported that the thickness of the electroreceptor epidermis varies throughout the body. The sensory cells themselves could also serve as a source of variation in capacitance. The apical surface of the receptor cells is thought to contribute to series capacitance whereas the basal surface is thought to affect membrane excitability as a 'typical' membrane capacitance in parallel with the resistance of the excitable membrane (Bennett, 1965; Bennett, 1971). The diameter of individual sensory cells within a KO only varies from 40 to 50 µm, but these cells are covered with branching microvilli that increase the surface area of each cell approximately 40-fold (Derbin and Szabo, 1968). Similarly, variation in the number of sensory cells per KO could also impact the capacitive properties of the receptor organ. The number of sensory cells per KO does indeed vary among the KOs within a single fish (Harder, 1968a). Like capacitance, resistance will be impacted by morphological features such as skin thickness, pore diameter and epithelial wall thickness.

Finally, studies of the axon initial segment have demonstrated that properties of voltage-gated ion channels such as location, distribution and inactivation kinetics play a pivotal role in the shape and timing of a spiking response, which contributes to electrical frequency tuning (Clark et al., 2009). This basic mechanism can also play a role in peripheral sensory tuning. For example, the amplitude of the current through mechanotransducer channels and the speed of adaptation covary with the best frequency of hair cells in the turtle cochlea, suggesting a role for variation in ion channel properties in generating frequency tuning (Ricci et al., 2003). Thus, there are multiple morphological and physiological features that could establish differences in sensory filtering across KOs, and thereby explain the observed covariation in frequency and duration tuning.

Implications for behavior

Pulse-type mormyrid electric fish use EODs for species recognition and mate choice (Arnegard et al., 2006; Feulner et al., 2009;

Hopkins and Bass, 1981; Machnik and Kramer, 2008). In *B. brachyistius*, males have longer EODs than females, and EOD duration correlates with relative dominance status among males (Carlson et al., 2000). Thus, long-pass filtering in the KO electrosensory system establishes a basic mechanism for distinguishing behaviorally relevant variation in conspecific EOD duration. However, there is extensive overlap in EOD duration among sympatric species (Arnegard et al., 2010; Carlson et al., 2011; Hopkins, 1981), suggesting the need to precisely distinguish small differences in duration. Further, EODs are individually distinctive (Friedman and Hopkins, 1996), and there is evidence that some species of mormyrids can use this information to discriminate between individuals (Graff and Kramer, 1992). Behavioral positioning during aggressive interactions maximizes the signal intensity experienced by receivers (Arnegard et al., 2006), possibly to maximize the discrimination of small temporal differences between waveforms. Precise temporal coding provides a robust mechanism for distinguishing slight variation in stimulus duration during overt behavioral interactions, whereas population coding provides a rough measure of stimulus duration at low intensities, when signaling fish are at a distance.

We tested natural EOD waveforms from 10 species as well as conspecific EOD waveforms subjected to temporal manipulations, and determined that the long-pass tuning we observed had clear effects on the detection of these behaviorally relevant stimuli (Fig. 7). Interestingly, for all measures tested, fish were more sensitive to heterospecific EODs of longer duration than conspecific EODs. This does not imply that the fish prefer heterospecific EODs that are longer in duration than conspecific EODs, only that they are more detectable at a given intensity. Our behavioral experiments provided a measure of signal detection, not preference, such as would be important in mate choice or intraspecific competition. Indeed, previous work has revealed clear behavioral preferences for conspecific EODs in several species (Arnegard et al., 2006; Feulner et al., 2009; Hopkins and Bass, 1981; Machnik and Kramer, 2008). Further, the early stages in the sensory pathway that we recorded from likely have less selectivity for specific waveforms compared with higher sensory regions. Thus, increases in either EOD amplitude or duration can increase the effective range of electric communication, but do not necessarily increase signal preference in specific behavioral contexts. Further, we found that threshold energy increased with increasing stimulus duration, likely because of the AC coupling of KOs. This suggests that greater energy is required to produce an equally detectable pulse of longer duration, which may place a limit on evolutionary increases in EOD duration. Thus, it will be interesting to determine how species diversity in EOD duration relates to diversity in EOD amplitude and energy, which will require carefully calibrated measurements in the field. It is possible that the evolution of increased EOD duration is compensated for by decreased EOD amplitude. Alternatively, variation in EOD duration may relate to diversity in the rates of EOD production, or to species differences in population density that place different selective pressures on signal range. It will also be interesting to relate variation in EOD duration, amplitude and energy to differences in KO physiology across species. The frequency tuning of KOs varies across species (Bass and Hopkins, 1984; Hopkins, 1981), suggesting that duration tuning will likely vary as well.

Relevance to other sensory systems

The use of multiple coding strategies is common in sensory systems (Lawhern et al., 2011). However, these distinct computations are often implemented in parallel sensory pathways that are specialized to extract information about different stimulus features (Carlson and Kawasaki, 2006; Nishino and Ohmori, 2009; Livingstone and Hubel, 1988; Sullivan and Konishi, 1984; Young, 1998). We demonstrate two distinct coding mechanisms in the sensory periphery operating at different ranges of intensities. Our findings are novel in revealing that both codes operate within the same circuit to extract information about the same stimulus feature, but work most effectively at different ranges of intensity. A combination of distinct coding schemes operating at different intensities may be used in other sensory systems as well.

We further demonstrate significant variability in peripheral tuning. Neural heterogeneity can increase the amount of information encoded in the activity of a population of central sensory neurons (Chelaru and Dragoi, 2008; Marsat and Maler, 2010). In contrast, redundancy, which exists at multiple stages of neural processing, can increase prediction accuracy and decrease ambiguity (Barlow, 1972; Barlow, 2001). Our results reveal that heterogeneity among peripheral sensory receptors allows for information processing through population coding. Heterogeneity in the frequency tuning of peripheral receptors may also be important for other temporal codes, such as the detection of interaural time differences (ITDs) in sound localization (Carr and Friedman, 1999). Indeed, monoaural inputs to ITD-detector neurons in barn owls vary in their spectrotemporal filtering properties, and this filtering has strong effects on ITD tuning (Fischer et al., 2011). Thus, the effects of spectrotemporal filtering at the periphery should be considered for a wide range of temporal codes.

Finally, our results reveal a basic mechanism by which sensory systems can determine stimulus duration even at low intensities, when the temporal precision of peripheral responses is severely degraded. Duration tuning in auditory systems is important for functions as varied as echolocation, acoustic communication, conspecific recognition and appreciation of music (Covey and Casseday, 1999). Duration-tuned neurons have been identified in the central auditory systems of echolocating bats as well as non-echolocating animals including frogs, rats, mice, guinea pigs, chinchillas and cats (Sayegh et al., 2011). In the mouse auditory midbrain, duration tuning is strongly dependent on other stimulus features, including intensity (Brand et al., 2000). We have demonstrated an intensity-dependent change in the peripheral code for duration. When analyzing central mechanisms for temporal processing, the diversity of peripheral responses and the importance of stimulus intensity should therefore be considered.

LIST OF SYMBOLS AND ABBREVIATIONS

a	tuning curve asymptote
BF	best frequency
BW_{10}	bandwidth
C_m	membrane capacitance of knollenorgans
C_s	series capacitance of knollenorgans
d	stimulus duration
ELa	anterior exterolateral nucleus
ELp	posterior exterolateral nucleus
EOD	electric organ discharge
I_t	threshold intensity
KO	knollenorgan
MS-222	tricaine methanesulfonate
nELL	electrosensory lateral line lobe
R_m	resistance of the membrane
R_s	resistance of the skin
V_m	voltage drop across the membrane
V_s	voltage drop across the skin
τ	tuning curve time constant

ACKNOWLEDGEMENTS

We thank Arielle Grossman and Chelsea Casareale for help with behavior experiments and knollenorgan recordings, respectively. We thank Dan Moran and Baranidharan Raman for help with modeling. We thank Jim Huettner for input on earlier versions of the manuscript.

FUNDING

This research was supported by the National Science Foundation [IOS-0818390 to B.A.C.], the National Institute on Deafness and Other Communication Disorders [F30-DC011197 to A.M.L.-W.] and the German Academic Exchange Service (fellowship to M.H.). Deposited in PMC for release after 12 months.

REFERENCES

Amagai, S. (1998). Time coding in the midbrain of mormyrid electric fish. II. Stimulus selectivity in the nucleus exterolateralis pars posterior. *J. Comp. Physiol. A* **182**, 131-143.

Amagai, S., Friedman, M. A. and Hopkins, C. D. (1998). Time coding in the midbrain of mormyrid electric fish. I. Physiology and anatomy of cells in the nucleus exterolateralis pars anterior. *J. Comp. Physiol. A* **182**, 115-130.

Arnegard, M. E. and Hopkins, C. D. (2003). Electric signal variation among seven blunt-snouted *Brienomyrus* species (Teleostei: Mormyridae) from a riverine species flock in Gabon, Central Africa. *Environ. Biol. Fishes* **67**, 321-339.

Arnegard, M. E., Bogdanowicz, S. M. and Hopkins, C. D. (2005). Multiple cases of striking genetic similarity between alternate electric fish signal morphs in sympatry. *Evolution* **59**, 324-343.

Arnegard, M. E., Jackson, B. S. and Hopkins, C. D. (2006). Time-domain signal divergence and discrimination without receptor modification in sympatric morphs of electric fishes. *J. Exp. Biol.* **209**, 2182-2198.

Arnegard, M. E., McIntyre, P. B., Harmon, L. J., Zelditch, M. L., Crampton, W. G., Davis, J. K., Sullivan, J. P., Lavoué, S. and Hopkins, C. D. (2010). Sexual signal evolution outpaces ecological divergence during electric fish species radiation. *Am. Nat.* **176**, 335-356.

Aubie, B., Becker, S. and Faure, P. A. (2009). Computational models of millisecond level duration tuning in neural circuits. *J. Neurosci.* **29**, 9255-9270.

Barlow, H. B. (1972). Single units and sensation: a neuron doctrine for perceptual psychology? *Perception* **1**, 371-394.

Barlow, H. B. (2001). Redundancy reduction revisited. *Network* **12**, 241-253.

Bass, A. H. and Hopkins, C. D. (1984). Shifts in frequency tuning of electroreceptors in androgen-treated mormyrid fish. *J. Comp. Physiol. A* **155**, 713-724.

Bell, C. C. (1990). Mormyromast electroreceptor organs and their afferent fibers in mormyrid fish. III. Physiological differences between two morphological types of fibers. *J. Neurophysiol.* **63**, 319-332.

Bell, C. C. and Grant, K. (1989). Corollary discharge inhibition and preservation of temporal information in a sensory nucleus of mormyrid electric fish. *J. Neurosci.* **9**, 1029-1044.

Bell, C. C. and Szabo, T. (1986). Electroreception in mormyrid fish: central anatomy. In *Electroreception* (ed. T. H. Bullock and W. Heiligenberg), pp. 375-421. New York: John Wiley and Sons.

Bennett, M. V. L. (1965). Electroreceptors in mormyrids. *Cold Spring Harb. Symp. Quant. Biol.* **30**, 245-262.

Bennett, M. V. L. (1971). Electroreception. In *Fish Physiology*, Vol. 5 (ed. W. S. Hoar and D. J. Randall), pp. 493-568. New York: Academic Press.

Brand, A., Urban, R. and Grothe, B. (2000). Duration tuning in the mouse auditory midbrain. *J. Neurophysiol.* **84**, 1790-1799.

Carlson, B. A. (2002). Electric signaling behavior and the mechanisms of electric organ discharge production in mormyrid fish. *J. Physiol. Paris* **96**, 405-419.

Carlson, B. A. (2006). A neuroethology of electrocommunication: senders, receivers, and everything in between. In *Communication in Fishes*, Vol. 2 (ed. F. Ladich, S. P. Collin, P. Moller and B. G. Kapoor), pp. 805-848. Enfield, NH: Science Publishers.

Carlson, B. A. (2009). Temporal-pattern recognition by single neurons in a sensory pathway devoted to social communication behavior. *J. Neurosci.* **29**, 9417-9428.

Carlson, B. A. and Hopkins, C. D. (2004). Stereotyped temporal patterns in electrical communication. *Anim. Behav.* **68**, 867-878.

Carlson, B. A. and Kawasaki, M. (2006). Ambiguous encoding of stimuli by primary sensory afferents causes a lack of independence in the perception of multiple stimulus attributes. *J. Neurosci.* **26**, 9173-9183.

Carlson, B. A. and Kawasaki, M. (2007). Behavioral responses to jamming and 'phantom' jamming stimuli in the weakly electric fish *Eigenmannia*. *J. Comp. Physiol. A* **193**, 927-941.

Carlson, B. A., Hopkins, C. D. and Thomas, P. (2000). Androgen correlates of socially induced changes in the electric organ discharge waveform of a mormyrid fish. *Horm. Behav.* **38**, 177-186.

Carlson, B. A., Hasan, S. M., Hollmann, M., Miller, D. B., Harmon, L. J. and Arnegard, M. E. (2011). Brain evolution triggers increased diversification of electric fishes. *Science* **332**, 583-586.

Carr, C. E. and Friedman, M. A. (1999). Evolution of time coding systems. *Neural Comput.* **11**, 1-20.

Chelaru, M. I. and Dragoi, V. (2008). Efficient coding in heterogeneous neuronal populations. *Proc. Natl. Acad. Sci. USA* **105**, 16344-16349.

Clark, B. D., Goldberg, E. M. and Rudy, B. (2009). Electrogenic tuning of the axon initial segment. *Neuroscientist* **15**, 651-668.

Covey, E. and Casseday, J. H. (1999). Timing in the auditory system of the bat. *Annu. Rev. Physiol.* **61**, 457-476.

Derbin, C. and Szabo, T. (1968). Ultrastructure of an electroreceptor (knollenorgan) in the mormyrid fish *Gnathonemus petersii*. I. *J. Ultrastruct. Res.* **22**, 469-484.

Edwards, C. J., Leary, C. J. and Rose, G. J. (2007). Counting on inhibition and rate-dependent excitation in the auditory system. *J. Neurosci.* **27**, 13384-13392.

Edwards, C. J., Leary, C. J. and Rose, G. J. (2008). Mechanisms of long-interval selectivity in midbrain auditory neurons: roles of excitation, inhibition, and plasticity. *J. Neurophysiol.* **100**, 3407-3416.

Feulner, P. G., Plath, M., Engelmann, J., Kirschbaum, F. and Tiedemann, R. (2009). Electrifying love: electric fish use species-specific discharge for mate recognition. *Biol. Lett.* **5**, 225-228.

Fischer, B. J., Steinberg, L. J., Fontaine, B., Brette, R. and Peña, J. L. (2011). Effect of instantaneous frequency glides on interaural time difference processing by auditory coincidence detectors. *Proc. Natl. Acad. Sci. USA* **108**, 18138-18143.

Fortune, E. S., Rose, G. J. and Kawasaki, M. (2006). Encoding and processing biologically relevant temporal information in electrosensory systems. *J. Comp. Physiol. A* **192**, 625-635.

Friedman, M. A. and Hopkins, C. D. (1996). Tracking individual mormyrid electric fish in the field using electric organ discharge waveforms. *Anim. Behav.* **51**, 391-407.

Friedman, M. A. and Hopkins, C. D. (1998). Neural substrates for species recognition in the time-coding electrosensory pathway of mormyrid electric fish. *J. Neurosci.* **18**, 1171-1185.

Gabbiani, F. and Koch, C. (1998). Principles of spike train analysis. In *Methods in Neuronal Modeling: From Ions to Networks* (ed. C. Koch and I. Segev), pp. 313-360. Cambridge, MA: MIT Press.

George, A. A., Lyons-Warren, A. M., Ma, X. and Carlson, B. A. (2011). A diversity of synaptic filters are created by temporal summation of excitation and inhibition. *J. Neurosci.* **31**, 14721-14734.

Graff, C. and Kramer, B. (1992). Trained weakly-electric fishes, *Pollimyrus isidori* and *Gnathonemus petersii* (Mormyridae, Teleostei) discriminate between waveforms of electric pulse discharges. *Ethology* **90**, 279-292.

Harder, W. (1968a). Die beziehungen zwischen elektrorezeptoren, elektrischem organ, seitenlinienorganen und nervensystem bei den Mormyridae (Teleostei, Pisces). *Z. Vgl. Physiol.* **59**, 272-318.

Harder, W. (1968b). Zum aufbau der epidermalen sinnesorgane der Mormyridae (Mormyriformes, Teleostei). *Z. Zellforsch. Mikrosk. Anat.* **89**, 212-224.

Hopkins, C. D. (1976). Stimulus filtering and electroreception: tuberous electroreceptors in three species of gymnotoid fish. *J. Comp. Physiol. A* **111**, 171-207.

Hopkins, C. D. (1981). On the diversity of electric signals in a community of mormyrid electric fish in West Africa. *Am. Zool.* **21**, 211-222.

Hopkins, C. D. and Bass, A. H. (1981). Temporal coding of species recognition signals in an electric fish. *Science* **212**, 85-87.

Köppl, C. (2009). Evolution of sound localisation in land vertebrates. *Curr. Biol.* **19**, R635-R639.

Lawhern, V., Nikonov, A. A., Wu, W. and Contreras, R. J. (2011). Spike rate and spike timing contributions to coding taste quality information in rat periphery. *Front. Integr. Neurosci.* **5**, 18.

Lissmann, H. W. and Mullinger, A. M. (1968). Organization of ampullary electric receptors in Gymnotidae (Pisces). *Proc. R. Soc. Lond. B* **169**, 345-378.

Livingstone, M. and Hubel, D. (1988). Segregation of form, color, movement, and depth: anatomy, physiology, and perception. *Science* **240**, 740-749.

Machnik, P. and Kramer, B. (2008). Female choice by electric pulse duration: attractiveness of the males' communication signal assessed by female bulldog fish, *Marcusenius pongolensis* (Mormyridae, Teleostei). *J. Exp. Biol.* **211**, 1969-1977.

Marsat, G. and Maler, L. (2010). Neural heterogeneity and efficient population codes for communication signals. *J. Neurophysiol.* **104**, 2543-2555.

Moller, P. and Bauer, R. (1973). 'Communication' in weakly electric fish, *Gnathonemus petersii* (Mormyridae) II. Interaction of electric organ discharge activities of two fish. *Anim. Behav.* **21**, 501-512.

Moller, P., Serrier, J. and Bowling, D. (1989). Electric organ discharge displays during social encounter in the weakly electric fish *Brienomyrus niger* L. (Mormyridae). *Ethology* **82**, 177-191.

Mugnaini, E. and Maler, L. (1987). Cytology and immunocytochemistry of the nucleus extrolateralis anterior of the mormyrid brain: possible role of GABAergic synapses in temporal analysis. *Anat. Embryol.* **176**, 313-336.

Neumann, E. and Nachmansohn, D. (1975). Nerve excitability – toward an integrating concept. In *Biomembranes*, Vol. 7 (ed. H. Eisenberg, E. Katchalski-Katzir and L. A. Manson), pp. 99-166. New York: Plenum Press.

Nishino, E. and Ohmori, H. (2009). The modulation by intensity of the processing of interaural timing cues for localizing sounds. *Mol. Neurobiol.* **40**, 157-165.

Nishino, E., Yamada, R., Kuba, H., Hioki, H., Furuta, T., Kaneko, T. and Ohmori, H. (2008). Sound-intensity-dependent compensation for the small interaural time difference cue for sound source localization. *J. Neurosci.* **28**, 7153-7164.

Paintner, S. and Kramer, B. (2003). Electrosensory basis for individual recognition in a weakly electric, mormyrid fish, *Pollimyrus adspersus* (Günther, 1866). *Behav. Ecol. Sociobiol.* **55**, 197-208.

Peña, J. L. and Konishi, M. (2000). Cellular mechanisms for resolving phase ambiguity in the owl's inferior colliculus. *Proc. Natl. Acad. Sci. USA* **97**, 11787-11792.

Post, N. and von der Emde, G. (1999). The "novelty response" in an electric fish: response properties and habituation. *Physiol. Behav.* **68**, 115-128.

Ricci, A. J., Crawford, A. C. and Fettiplace, R. (2003). Tonotopic variation in the conductance of the hair cell mechanotransducer channel. *Neuron* **40**, 983-990.

Rose, G. J. (2004). Insights into neural mechanisms and evolution of behaviour from electric fish. *Nat. Rev. Neurosci.* **5**, 943-951.

Sawtell, N. B., Williams, A. and Bell, C. C. (2005). From sparks to spikes: information processing in the electrosensory systems of fish. *Curr. Opin. Neurobiol.* **15**, 437-443.

Sayegh, R., Aubie, B. and Faure, P. A. (2011). Duration tuning in the auditory midbrain of echolocating and non-echolocating vertebrates. *J. Comp. Physiol. A* **197**, 571-583.

Sullivan, J. P., Lavoué, S. and Hopkins, C. D. (2002). Discovery and phylogenetic analysis of a riverine species flock of African electric fishes (Mormyridae: Teleostei). *Evolution* **56**, 597-616.

Sullivan, W. E. and Konishi, M. (1984). Segregation of stimulus phase and intensity coding in the cochlear nucleus of the barn owl. *J. Neurosci.* **4**, 1787-1799.
Szabo, T. (1965). Sense organs of the lateral line system in some electric fish of the Gymnotidae, Mormyridae and Gymnarchidae. *J. Morphol.* **117**, 229-249.
Szabo, T., Enger, P. S. and Libouban, S. (1979). Electrosensory systems in the mormyrid fish, *Gnathonemus petersii*: special emphasis on the fast conducting pathway. *J. Physiol. Paris* **75**, 409-420.
Szamier, R. B. and Wachtel, A. W. (1970). Special cutaneous receptor organs of fish. VI. Ampullary and tuberour organs of *Hypopomus*. *J. Ultrastruct. Res.* **30**, 450-471.
Szabo, T., Ravaille, M., Libouban, S. and Enger, P. S. (1983). The mormyrid rhombencephalon: I. Light and EM investigations on the structure and connections of the lateral line lobe nucleus with HRP labelling. *Brain Res.* **266**, 1-19.
Szűcs, A. (1998). Applications of the spike density function in analysis of neuronal firing patterns. *J. Neurosci. Methods* **81**, 159-167.
von der Emde, G. (1999). Active electrolocation of objects in weakly electric fish. *J. Exp. Biol.* **202**, 1205-1215.
Xu-Friedman, M. A. and Hopkins, C. D. (1999). Central mechanisms of temporal analysis in the knollenorgan pathway of mormyrid electric fish. *J. Exp. Biol.* **202**, 1311-1318.
Young, E. D. (1998). Parallel processing in the nervous system: evidence from sensory maps. *Proc. Natl. Acad. Sci. USA* **95**, 933-934.
Zakon, H. H. (1986). The electroreceptive periphery. In *Electroreception* (ed. T. H. Bullock and W. Heiligenberg), pp. 103-156. New York: John Wiley and Sons.
Zakon, H. H. (2003). Insight into the mechanisms of neuronal processing from electric fish. *Curr. Opin. Neurobiol.* **13**, 744-750.